RESEARCH ARTICLE

Effects of Wall Speed Ratio and Magnetic Field on MHD Mixed Convection of CuO-Water Nanofluid in a Square Cavity

A. Shamadhani Begum[1], **R. J. Punith Gowda**[2], **Mahendrasinh R. Chauhan**[3] **and Muhammad Ijaz Khan**[4,*]

[1] Department of Mathematics, Rathinam Global Deemed to be University, Coimbatore, Tamil Nadu, India
[2] Department of Mathematics, Bapuji Institute of Engineering & Technology, Davangere 577004, India
[3] Department of Mechanical Engineering, Gokul Global University, Siddhpur, Gujarat, India
[4] Department of Mechanical Engineering, College of Engineering, Prince Mohammad Bin Fahd University, Al-Khobar, Saudi Arabia

Abstract

The effect of wall speed ratios on magnetohydrodynamic (MHD) mixed convective flow in a square cavity filled with CuO-water nanofluid, incorporating a diagonally moving heated/cooled wall, is examined. The governing equations, which account for magnetic field effects, buoyancy forces, and nanoparticle concentration, are solved numerically using the finite volume method with the SIMPLE algorithm. The study investigates the effects of wall speed ratios (γ = 0, 1, 2), Richardson numbers (Ri = 0.1, 1, 10), Hartmann numbers (Ha = 0, 10, 25, 50), and nanoparticle volume fractions (ϕ = 0.0, 0.05) on flow behavior and convective heat transfer within the cavity. The results demonstrate that the wall speed ratio strongly influences streamline patterns and heat transfer. Increasing the wall speed ratio (γ = 0–2) enhances heat transfer by up to 476% at low Ri, while nanoparticle addition improves it by 11–18%. In contrast, increasing the Hartmann number (Ha = 0–50) suppresses convection and reduces heat transfer by 8–16% due to magnetic damping. These findings identify optimal wall speed ratios for maximizing thermal performance, highlighting the importance of tailored flow control strategies in MHD nanofluid engineering applications. These findings have significant implications for thermal management design in applications such as heat exchangers, electronic cooling systems, and energy storage devices.

Keywords: diagonally moving wall, magnetohydrodynamics (MHD), mixed convection, nanofluid, cavity.

Submitted: 23 May 2026
Revised: 23 June 2026
Accepted: 08 July 2026
Published: 13 August 2026

Vol. 2, **No.** 3, 2026.
10.62762/IJTSSE.2026.135135

***Corresponding author:**
Muhammad Ijaz Khan
ijzfmg_khan@yahoo.com

Citation
Begum, A. S., Gowda, R. J. P., Chauhan, M. R., & Khan, M. I. (2026). Effects of Wall Speed Ratio and Magnetic Field on MHD Mixed Convection of CuO-Water Nanofluid in a Square Cavity. *International Journal of Thermo-Fluid Systems and Sustainable Energy*, 2(3), 101–116.

Nomenclature

Symbol	Description
B_0	Applied magnetic flux density (T)
c_p	Fluid specific heat (J/(kg K))
d_p	Particle diameter (nm)
Gr	Grashof number
g	Gravitational acceleration $(\mathrm{m/s^2})$
H	Height of the enclosure (m)
Ha	Hartmann number
k	Thermal conductivity (W/(m K))
L	Width of the enclosure (m)
Nu	Local Nusselt number
$\overline{Nu}$	Average Nusselt number
p	Pressure $(\mathrm{N/m^2})$
P	Dimensionless pressure
Pr	Prandtl number
Re	Reynolds number
Ri	Richardson number
t	Time (s)
T	Dimensionless temperature
T_0	Reference temperature (273 K)
V	Constant velocity (m/s)
u, v	Velocity components (m/s)
U, V	Dimensionless velocity components
x, y	Cartesian coordinates (m)
X, Y	Dimensionless Cartesian coordinates
α	Thermal diffusivity $(\mathrm{m^2/s})$
β	Thermal expansion coefficient (1/K)
φ	Solid volume fraction
κ	Boltzmann constant $(1.381\times10^{-23}\,\mathrm{J/K})$
γ	Wall speed ratio
μ	Dynamic viscosity $(\mathrm{N\,s/m^2})$
ν	Kinematic viscosity $(\mathrm{m^2/s})$
θ	Temperature
ρ	Density of the working fluid $(\mathrm{kg/m^3})$
σ	Heat capacity ratio of nanofluid
σ_f, σ_{nf}	Electrical conductivity of base fluid and nanofluid (S/m)
τ	Dimensionless time

Subscripts

Subscript	Description
c	Cold wall
h	Hot wall
l	Left wall
r	Right wall
f	Base fluid
p	Solid particle
nf	Nanofluid

1 Introduction

Investigating mixed convection in open and closed cavities is crucial due to its broad applications in industrial and engineering sectors, encompassing heat exchangers, electronic cooling, nuclear reactors, solar technologies, and air conditioning. Evaluating the performance of various cooling systems poses a complex challenge in thermal engineering. To enhance the efficiency of thermal equipment through diverse mechanisms, extensive numerical and experimental research has been conducted over the past few decades, including optimizing design, exploring innovative heat transfer fluids, and developing new mathematical models. Additionally, significant attention has been devoted to understanding the impact of magnetic fields on natural and mixed convection, highlighting their crucial role in governing convective flows and thermal behavior in engineering applications.

Mixed convection flows, also known as combined free and forced convection flows, are commonly observed in various technological, industrial, and natural phenomena. Examples include solar receivers subjected to wind currents, electronic devices cooled by fans, nuclear power plants cooled during critical shutdown, heat exchangers operating in low-velocity environments, and flows in the ocean and atmosphere. The heat and mass transfer of nanofluids in enclosures has been the subject of extensive numerical investigation. However, research on the natural and mixed convection of nanofluids in horizontal and vertical channels remains limited. Mixed convection—a complex phenomenon central to heat transfer processes—arises from the interaction between shear flow induced by moving surfaces and thermal buoyancy. Understanding this interaction, commonly observed in lid-driven enclosures, is key to enhancing flow mixing and heat transfer efficiency. The geometry of a lid-driven enclosure, with its simple shape and regular boundary conditions, lends itself well to flow and thermal field simulations.

Several authors have examined moving-wall configurations in MHD nanofluid systems. Selimefendigil and Öztop [1] demonstrated that in a lid-driven square cavity filled with nanofluid, moving wall motion combined with a magnetic field considerably alters flow circulation and heat transfer, with heat transfer increasing by 17% at higher Richardson numbers while decreasing with increasing Hartmann number. Gibanov et al. [2] showed that wall-driven motion combined with an inclined magnetic field efficiently regulates momentum and heat transfer in nanofluid-filled enclosures, where higher Hartmann numbers cause systematic suppression of convection. Alsabery et al. [3] demonstrated that wall motion significantly modifies the flow structure and boundary layer characteristics in MHD nanofluid-filled square cavities, with the magnetic field strength and nanoparticle volume fraction jointly governing the thermal performance. Begum et al. [4] discovered that in a cavity filled with nanofluid, magnetic fields and a lid that moves diagonally improve thermal transport while altering the flow pattern. Selimefendigil and Öztop [5] modeled and optimized MHD mixed convection in a lid-driven trapezoidal cavity filled with alumina–water nanofluid, demonstrating that the choice of electrical conductivity model significantly alters the predicted heat transfer rate and that higher Hartmann numbers consistently suppress convective transport. Nithyadevi et al. [6] investigated mixed convection induced by a uniformly heated moving lid positioned at the center of a non-Darcian porous enclosure filled with nanofluid, exploring various wall speed ratios, with nonlinear (sinusoidal-pattern) heating applied to the vertical walls. Their results indicated that the centrally located moving lid significantly enhanced the heat transfer rate by 92.5%, surpassing conventional moving-boundary lids, with heat transfer performance further improving at higher nanoparticle volume fractions.

Magnetohydrodynamics (MHD) finds extensive application across several industrial sectors, including MHD power generators, cooling systems for nuclear reactors, bearings, micro-MHD pumps, and boundary layer control. The presence of a magnetic field and an electrically conductive liquid has a substantial impact on hydrodynamic boundary layers, as seen in technological systems involving liquid metal and plasma flow subjected to a transverse magnetic field. Several recent studies have focused on boundary layer flow in transverse configurations under magnetic field influence. Bahoum et al. [7] analyzed mixed MHD convection in a lid-driven cubic cavity filled with hybrid nanofluid, demonstrating that increasing Reynolds, Richardson, and nanoparticle fractions improves heat transfer, while higher Hartmann numbers suppress it. Similarly, Toghraie [8] explored the influence of cavity tilt, Hartmann number, and nanoparticle volume fraction on Cu–water nanofluid in a trapezoidal lid-driven cavity, highlighting the sensitivity of flow to geometry. Hosseinzadeh et al. [9] studied hybrid nanofluid flow in an octagonal porous cavity under the influence of magnetic field and radiation, demonstrating that increasing the magnetic field strength effectively suppresses velocity components and reduces convective circulation, while nanoparticle loading enhances the overall thermal performance. Oztop et al. [10] examined MHD mixed convection in a lid-driven square cavity with a corner heater, demonstrating that increasing the Hartmann number reduces fluid velocity and suppresses convective heat transfer, while the location and size of the corner heater significantly influence the flow structure and Nusselt number distribution. Hussain et al. [11] analyzed MHD mixed convection and entropy generation of water–alumina nanofluid in a double lid-driven cavity with discrete heating, showing that the applied magnetic field suppresses fluid velocity through Lorentz damping and that nanoparticle addition enhances the Nusselt number, particularly at higher Reynolds numbers. Shah et al. [12] demonstrated that an inclined magnetic field modifies the flow pattern and enhances heat and mass transfer. Mehmood et al. [13] numerically simulated MHD mixed convection in an alumina–water nanofluid filled square porous cavity using the KKL model, finding that the inclined magnetic field suppresses convective velocity through the Lorentz force and that non-linear thermal radiation and nanoparticle volume fraction jointly determine the average Nusselt number. Hussain et al. [14] numerically examined the effects of inclination angle on mixed convective nanofluid flow in a double lid-driven cavity with discrete heat sources, revealing that the inclination angle and Hartmann number jointly govern the flow structure and that nanoparticle addition consistently improves the heat transfer rate.

Recent investigations have demonstrated that oscillating magnetic fields play a crucial role in governing nanofluid velocity and thermal transport characteristics, with field dynamics significantly modifying the flow behavior even at moderate intensities [15]. Asghar et al. [16] examined magnetized hybrid nanofluid flow under mixed convection, considering the combined effects of velocity slip and heat source/sink. When a magnetic field is applied to a conducting fluid—such as a nanofluid containing metal nanoparticles—it interacts with the fluid's motion, influencing flow characteristics such as velocity and temperature distribution through magnetohydrodynamic (MHD) effects.

Sivasankaran et al. [17] demonstrated that hydromagnetic combined convection in a lid-driven cavity with sinusoidal boundary conditions on both sidewalls is strongly influenced by the magnetic field strength and phase deviation, with the Hartmann number playing a decisive role in suppressing convective circulation and modifying the Nusselt number distribution. Sheikholeslami et al. [18] simulated MHD CuO–water nanofluid flow and convective heat transfer under Lorentz forces, showing that the magnetic field retards fluid velocity and that Nusselt number decreases with increasing Hartmann number, while nanoparticle volume fraction enhances heat transfer. Elshehabey and Ahmed [19] investigated MHD mixed convection in a lid-driven cavity filled with nanofluid using Buongiorno's model with sinusoidal temperature distributions on both vertical walls, finding that increasing the Hartmann number suppresses convection while increasing the nanoparticle volume fraction and Reynolds number enhances heat and mass transfer rates.

Begum et al. [20] investigated Cu–water nanofluid flow in a rectangular, porous-media-filled enclosure under an inclined magnetic field, analyzing mixed convective heat transfer under varying Hartmann numbers and magnetic field orientations. Their results showed that increasing the Hartmann number and altering the magnetic field direction suppress convection and promote a shift toward conduction-dominated heat transfer. Nithyadevi and Begum [21] further examined the effect of a mid-horizontal moving lid in a square porous enclosure filled with Cu–water nanofluid using the Brinkman–Forchheimer extended Darcy model, finding that decreasing the Darcy number and increasing the Richardson number reduce the average Nusselt number, with the porous medium significantly enhancing conduction. Taamneh and Bataineh [22] demonstrated that Nusselt numbers in square lid-driven cavities filled with Al_2O_3–water nanofluid increase with both the Richardson number and particle volume fraction. Similarly, Chowdhury and Alim [23] analyzed mixed convection in double lid-driven wavy cavities using hybrid nanofluids, revealing that wavy walls enhance heat transfer while magnetic fields suppress it. Chamkha and Abu-Nada [26] further showed that the choice of viscosity model significantly affects the predicted heat transfer rate in nanofluid-filled lid-driven cavities, emphasizing the importance of accurate thermophysical property modeling.

Compared with conventional fluids, nanofluids exhibit substantially improved thermal conductivity and higher heat transfer efficiency. Nanofluids play an essential role across many engineering domains and real-world applications, including heat exchangers, cooling systems, and nuclear reactors. Hanif et al. [24] investigated the use of Ag–TiO_2 nanoparticles to improve heat transfer in a slanted cavity in the presence of thermal radiation and a magnetic field, finding that the magnetic field orientation relative to the flow direction determines whether convective currents are dampened or enhanced, thereby altering the temperature distribution and heat transfer rate. Sarlak et al. [25] studied laminar flow of a water/SWCNT nanofluid in a triangular cavity involving cold-liquid injection for convective heat exchange. Nazir et al. [27] analyzed the impact of heat generation and radiative heat flux on the convective motion of nanofluid within a porous triangular cavity under thermal boundary conditions. Nanofluids typically enhance heat transfer owing to their higher thermal conductivity; when combined with radiative heat flux and internal heat generation, the resulting heat transfer mechanisms become more complex and can lead to improved overall performance, depending on the specific conditions. Qureshi et al. [28] examined the flow of a hybrid nanoliquid across a horizontal channel containing a cavity, showing that the Hartmann number and cavity geometry significantly influence both heat transfer rates and hydrodynamic forces.

Gowthaman et al. [29] further confirmed that plate speed and nanoparticle loading jointly govern shear- and buoyancy-dominated heat transfer in cavity configurations, underscoring the significance of wall motion as a thermal control parameter. In a recent study [30], researchers explored MHD mixed convection and entropy generation in a lid-driven square cavity under the influence of inclined magnetic fields imposed on its upper and lower diagonal triangular domains. This research highlighted how magnetic fields and nanoparticle concentrations impact thermal efficiency. Nonetheless, the study did not systematically vary the wall speed ratio, nor did it examine the combined effects of wall speed ratio, Hartmann number, Richardson number, and nanofluids on optimizing heat transfer. The current research builds on this by conducting an extensive parametric analysis of these interacting factors to pinpoint the conditions that enhance thermal performance to the fullest.

2 Novelty

In recent research efforts, numerical simulations have focused on enhancing thermal equipment efficiency through various means such as improved design, innovative heat transfer fluids, and the development of new mathematical models. One promising approach involves using moving insert devices that scrape the surfaces of heat exchangers. While traditional lid-driven cavity research focuses on horizontal or vertical wall motion, diagonal actuation introduces complexity and anisotropy to the flow structure. This method addresses several challenges encountered across different sectors. Notably, it lessens the requirement for bigger heat exchangers to make up for fouling-induced reductions in heat transmission. The use of moving scrapers enables continuous operation in sectors like chemical and food processing, eliminating downtime that would otherwise impact plant productivity. Moreover, heating a uniformly mixed fluid ensures a consistent temperature field within the fluid, which is crucial for maintaining quality, particularly in the food industry. By examining such diagonal motion under mixed thermal conditions in a novel manner, this study offers new insights on flow manipulation and heat transfer management in square cavities.

Another area of study explores the influence of magnetic fields on convective flow and thermal behaviors in enclosures filled with nanofluids. This research is pivotal for controlling convective heat transfer in various engineering applications.

2.1 Application Prospects of the Present Study

The insights of the current study have extensive technical implications, particularly in areas where good heat control is critical. The findings may be used to the design of modern electronic cooling systems, compact heat exchangers, and energy storage devices, where accurate heat transfer improves performance and dependability. Magnetically controlled nanofluid flows can help regulate temperature in medical devices and medicinal treatments. Similarly, the findings apply to microfluidic and lab-on-chip systems, where effective mixing and temperature homogeneity are critical. Applications include nuclear and renewable energy systems, as well as aerospace technology, where high magnetic fields and intense heat flows demand efficient cooling solutions. Furthermore, modern manufacturing processes such as semiconductor fabrication, additive manufacturing, and crystal growth can benefit from enhanced convection control due to the combined effects of nanofluids, wall motion, and magnetic fields.

3 Mathematical formulation

Figure 1 illustrates a two-dimensional square cavity with dimensions height H and length L. The left side of the cavity is maintained at temperature T_h for heating, while the opposite side is cooled to temperature T_c. The other two sides of the cavity are adiabatic. Inside the cavity, there is a diagonal wall moving at a constant velocity γV, also heated/cooled to temperature T_h/T_c. This setup induces mixed convection due to both thermal buoyancy forces and the movement of the diagonal wall. Additionally, a uniform magnetic field B_0 is applied perpendicular to the buoyancy force in a Cartesian coordinate system.

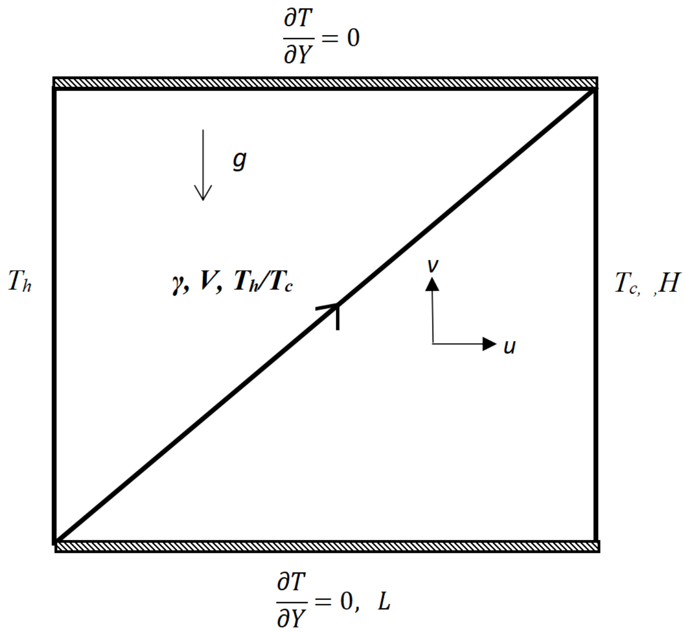

Figure 1. Physical configuration.

To enhance heat transfer characteristics, CuO nanoparticles are dispersed in water, forming a nanofluid that conforms to the Boussinesq approximation for fluid properties, with the exception of density variations. The nanofluid maintains consistent thermophysical properties throughout this investigation. The flow is considered to be laminar, Newtonian, and incompressible, without accounting for effects such as viscous dissipation, internal heat generation, or radiation heat transfer.

3.1 Governing Equations

With the above-mentioned assumptions, the governing equations for the magnetohydrodynamic nanofluid-filled cavity can be written as follows [31].

$$\frac{\partial u}{\partial x} + \frac{\partial v}{\partial y} = 0.$$

$$\frac{\partial u}{\partial t}+\left(u\frac{\partial u}{\partial x}+v\frac{\partial u}{\partial y}\right)=-\frac{1}{\rho_{nf}}\frac{\partial p}{\partial x}+\nu_{nf}\left(\frac{\partial^2 u}{\partial x^2}+\frac{\partial^2 u}{\partial y^2}\right).$$

$$\frac{\partial v}{\partial t}+\left(u\frac{\partial v}{\partial x}+v\frac{\partial v}{\partial y}\right)=-\frac{1}{\rho_{nf}}\frac{\partial p}{\partial y}+\nu_{nf}\left(\frac{\partial^2 v}{\partial x^2}+\frac{\partial^2 v}{\partial y^2}\right)+g\beta_{nf}(\theta_h-\theta_c)+\frac{-\sigma_{nf}B_0^2 v}{\rho_{nf}}.$$

$$\sigma\frac{\partial \theta}{\partial t}+\left(u\frac{\partial \theta}{\partial x}+v\frac{\partial \theta}{\partial y}\right)=\alpha_{nf}\left(\frac{\partial^2 \theta}{\partial x^2}+\frac{\partial^2 \theta}{\partial y^2}\right).$$

By introducing specific parameters, the dimensional governing equations are transformed into non-dimensional equations, aligning with the assumptions and requirements of the problem.

$$X=\frac{x}{L},\quad Y=\frac{y}{L},\quad U=\frac{u}{U_0},\quad V=\frac{v}{U_0},$$
$$P=\frac{p}{\rho_{nf}U_0^2},\quad \tau=\frac{U_0 t}{L},\quad T=\frac{\theta-\theta_c}{\theta_h-\theta_c},\quad \theta_h>\theta_c.$$

The dimensional governing equations are transformed into non-dimensional equations by introducing the following characteristic parameters:

$$Gr=\frac{g\beta_f(\theta_h-\theta_c)L^3}{\nu_f^2},\qquad Pr=\frac{\nu_f}{\alpha_f},$$
$$Re=\frac{U_0 L}{\nu_f},\qquad Ri=\frac{Gr}{Re^2},$$
$$\sigma=\frac{\varepsilon(\rho c_p)_f+(1-\varepsilon)(\rho c_p)_p}{(\rho c_p)_f}.$$

Consequently, the dimensionless governing equations are expressed as follows [32]:

$$\frac{\partial U}{\partial X}+\frac{\partial V}{\partial Y}=0. \tag{1}$$

$$\frac{\partial U}{\partial \tau}+\left(U\frac{\partial U}{\partial X}+V\frac{\partial U}{\partial Y}\right)=-\frac{\partial P}{\partial X}+\frac{\nu_{nf}}{\nu_f}\frac{1}{Re}\nabla^2 U. \tag{2}$$

$$\frac{\partial V}{\partial \tau}+\left(U\frac{\partial V}{\partial X}+V\frac{\partial V}{\partial Y}\right)=-\frac{\partial P}{\partial Y}+\frac{\nu_{nf}}{\nu_f}\frac{1}{Re}\nabla^2 V+\frac{\beta_{nf}}{\beta_f}Ri\,T-\frac{\rho_f}{\rho_{nf}}\frac{\sigma_{nf}}{\sigma_f}\frac{Ha^2}{Re}. \tag{3}$$

$$\sigma\frac{\partial T}{\partial \tau}+U\frac{\partial T}{\partial X}+V\frac{\partial T}{\partial Y}=\frac{\alpha_{nf}}{\alpha_f}\frac{1}{Pr\,Re}\nabla^2 T. \tag{4}$$

For simplification, the thermophysical properties of the nanofluid are assumed to remain uniform and constant throughout the flow domain.

3.1.1 *Properties of Nanofluid*

Table 1. Thermo-physical properties of base fluid (water) and CuO.

	ρ (kg/m^3)	C_p (J/kg·K)	k (W/m·K)	β (1/K)	d_p (nm)
Base fluid	997.1	4179.0	0.613	2.1×10^{-4}	–
CuO	6500.0	540.0	18.0	0.85×10^{-5}	29

Thermophysical properties of the base fluid and CuO nanoparticles are listed in Table 1. The effective density, thermal diffusivity, heat capacity, and thermal expansion coefficient of the nanofluid are expressed as

$$\begin{cases}\rho_{nf}=(1-\phi)\rho_f+\phi\rho_p,\\ \alpha_{nf}=\dfrac{k_{nf}}{(\rho c_p)_{nf}},\\ (\rho c_p)_{nf}=(1-\phi)(\rho c_p)_f+\phi(\rho c_p)_p,\\ (\rho\beta)_{nf}=(1-\phi)(\rho\beta)_f+\phi(\rho\beta)_p.\end{cases} \tag{5}$$

where the subscripts f, p, and nf denote the base fluid, solid particle, and nanofluid, respectively.

The effective thermal conductivity model proposed by Koo and Kleinstreuer [33] consists of a conventional static component and a Brownian motion component. The model accounts for the effects of particle diameter (d_p), nanoparticle volume fraction (ϕ), and temperature (T), and is written as

$$k_{nf}=k_{\text{static}}+k_{\text{Brownian}}. \tag{6}$$

The static thermal conductivity is determined using the Maxwell–Garnett model [34],

$$k_{\text{static}}=k_f\left[\frac{k_p+2k_f-2\phi(k_f-k_p)}{k_p+2k_f+\phi(k_f-k_p)}\right]. \tag{7}$$

The Brownian-motion contribution is evaluated using the empirical functions β and $f(T,\phi)$, which account for the hydrodynamic interaction between nanoparticles and the temperature effect:

$$k_{\text{Brownian}} = 5 \times 10^4 \, \beta \, \phi \, \rho_f \, c_{p,f} \sqrt{\frac{\kappa T}{\rho_p d_p}} \, f(T,\phi). \tag{8}$$

where

$$\beta = 0.0011(100\phi)^{-0.7272}, \tag{9}$$

and

$$f(T,\phi) = (-6.04\phi + 0.4705)T + (1722.3\phi - 134.63), \tag{10}$$

with

$$293 \text{ K} < T < 325 \text{ K}, \qquad 1\% < \phi < 4\%.$$

Vajjha and Das [35] improved the Koo and Kleinstreuer model [33] by incorporating extensive experimental data over a wider temperature range (298–363 K) and a broader range of nanoparticle volume fractions. Their results showed that the thermal conductivity of nanofluids increases with increasing temperature and particle concentration, whereas it decreases with increasing particle diameter. The resulting correlation provides more accurate predictions of the effective thermal conductivity over a wide range of operating conditions.

Accordingly, the effective thermal conductivity is expressed as

$$\begin{aligned} k_{nf} = k_f \left[\frac{k_p + 2k_f - 2\phi(k_f - k_p)}{k_p + 2k_f + \phi(k_f - k_p)} \right] \\ + 5 \times 10^4 \, \beta \, \phi \, \rho_f \, c_{p,f} \sqrt{\frac{\kappa T}{\rho_p d_p}} \, f(T,\phi). \end{aligned} \tag{11}$$

where

$$\begin{aligned} f(T,\phi) = \left(2.8217 \times 10^{-2}\phi + 3.917 \times 10^{-3}\right) \left(\frac{T}{T_0}\right) \\ + \left(-3.0669 \times 10^{-2}\phi - 3.91123 \times 10^{-3}\right), \end{aligned} \tag{12}$$

and

$$\beta = 9.881(100\phi)^{-0.9446}, \tag{13}$$

which is valid for

$$298 \text{ K} < T < 363 \text{ K}, \qquad 1\% < \phi < 6\%.$$

For the pure base fluid case ($\phi = 0$), the standard thermophysical properties of water are used directly.

The effective viscosity of the nanofluid is also modified by the Brownian-motion effect and is expressed as

$$\mu_{nf} = \mu_{\text{static}} + \mu_{\text{Brownian}}. \tag{14}$$

The total effective viscosity is calculated as

$$\mu_{nf} = \frac{\mu_f}{(1-\phi)^{2.5}} + \left(\frac{k_{\text{Brownian}}}{k_f}\right)\left(\frac{\mu_f}{Pr_f}\right). \tag{15}$$

In the present study, the Vajjha–Das model is adopted to determine the effective thermal conductivity and viscosity of the nanofluid, as it provides improved prediction accuracy under elevated-temperature conditions. The model accounts for both the conventional static contribution and the dynamic contribution induced by Brownian motion, while considering the effects of particle diameter (d_p), particle volume fraction (ϕ), and temperature (T).

Accordingly,

$$k_{nf} = k_{\text{static}} + k_{\text{Brownian}}. \tag{16}$$

3.2 Boundary conditions

The dimensionless initial and boundary conditions are given as

$$\begin{array}{lll} U = V = 0, & T = T_h, & X = 0, \\ U = V = 0, & T = T_c, & X = 1, \\ U = V = 0, & \dfrac{\partial T}{\partial Y} = 0, & Y = 0, \\ U = V = 0, & \dfrac{\partial T}{\partial Y} = 0, & Y = 1, \\ U(i,j) = V(i,j) = \gamma V, & T = T_h \text{ or } T_c, & i = j. \end{array} \tag{17}$$

The average Nusselt number along the heated vertical wall is obtained by integrating the local Nusselt number. The continuity of the heat flux at the solid–nanofluid interface is expressed as

$$k_{nf}\left(\frac{\partial T}{\partial n}\right)_{nf} = k_s\left(\frac{\partial T}{\partial n}\right)_s. \tag{18}$$

Accordingly, the average Nusselt number is defined as

$$Nu_{\text{avg}} = -\left.\frac{k_{nf}}{k_f}\frac{\partial T}{\partial X}\right|_{X=0}. \tag{19}$$

3.3 Numerical Solution

The finite volume method (FVM) is employed to discretize the dimensionless governing equations. The convection terms are discretized using the power-law scheme, which provides a close approximation to the exact solution. A staggered grid arrangement is adopted within the computational domain, in which the scalar variables (P and T) are stored at the cell centers, whereas the velocity components (U and V) are defined at the control volume faces. The coupled continuity and momentum equations are solved using the Semi-Implicit Method for Pressure-Linked Equations (SIMPLE) algorithm [36]. The under-relaxation factors are set to 0.2 for U, 0.2 for V, and 0.5 for P. The resulting system of linear algebraic equations is solved using the Tri-Diagonal Matrix Algorithm (TDMA) with a line-by-line iterative procedure until convergence is achieved. The convergence criterion applied to all dependent variables is given by

$$\frac{\sum_{i,j} \left| \phi_{i,j}^{n+1} - \phi_{i,j}^{n} \right|}{\sum_{i,j} \left| \phi_{i,j}^{n+1} \right|} < 10^{-5}. \tag{20}$$

Here, ϕ represents the dependent variable (U, V, or T), while i and j denote the spatial indices and n represents the iteration level. Unless otherwise specified, the convergence tolerance is fixed at 10^{-5} throughout all simulations.

All computations were performed on a computer equipped with an AMD Ryzen 3 7320U processor (2.40 GHz), 8 GB RAM, and a 64-bit operating system. The typical computational time required to obtain a converged solution was approximately 4×10^3 s.

3.4 Code Validation

A two-dimensional in-house computational code was developed to solve the present problem. To verify the numerical accuracy of the proposed method, a grid independence study was conducted using five different grid resolutions, ranging from 41×41 to 181×181, as listed in Table 2. Based on the grid independence analysis, a mesh size of 141×141 was selected for all subsequent simulations, providing a satisfactory compromise between computational accuracy and efficiency.

To further validate the numerical model, the present results were compared with the benchmark solutions reported by Jmai *et al.* [37], who investigated mixed convection in a square cavity with different wall velocity ratios (γ). In addition, the streamline and isotherm contours shown in Figure 2(b) were compared with the results reported by Kefayati *et al.* [38] to verify the implementation of the magnetic field effect. Excellent agreement is observed between the present predictions and the published numerical results, confirming the accuracy and reliability of the proposed numerical model.

Table 2. Grid independence study over the average Nusselt number with $\gamma = 0$, $Ha = 10$, $Ri = 1$ and $\varphi = 0.0$.

Grid	$\overline{Nu}_{avg}$
41×41	2.52461
61×61	2.94125
81×81	3.49876
101×101	4.00021
121×121	4.10001
141×141	4.10286
161×161	4.10399
181×181	4.10402

Furthermore, Figure 2(c) compares the present diagonal moving-wall configuration with the conventional horizontal moving-wall cavity studied by Sheremet and Pop [32]. The comparison demonstrates that the diagonal wall motion adopted in the present study enhances the overall heat transfer performance.

Therefore, the above validation studies provide confidence in the accuracy and reliability of the numerical methodology employed in the subsequent analysis.

4 Results and Discussions

The effects of the wall speed ratio on magnetohydrodynamic mixed convection in a diagonally lid-driven nanofluid-filled cavity are investigated numerically. The primary objective of this study is to identify the operating conditions that maximize the heat transfer performance. A comprehensive parametric study is carried out by varying the Richardson number (Ri = 0.1, 1, and 10), Hartmann number ($Ha = 0, 10, 25$, and 50), wall speed ratio ($\gamma = 0, 1$, and 2), and nanoparticle volume fraction ($\phi = 0$ and 0.05), while keeping the Prandtl number fixed at $Pr = 6.2$.

The numerical results are analyzed in terms of the temperature field, flow structure, velocity distribution, and average Nusselt number. Particular attention is paid to the coupled effects of buoyancy, magnetic field strength, wall motion, and nanoparticle concentration

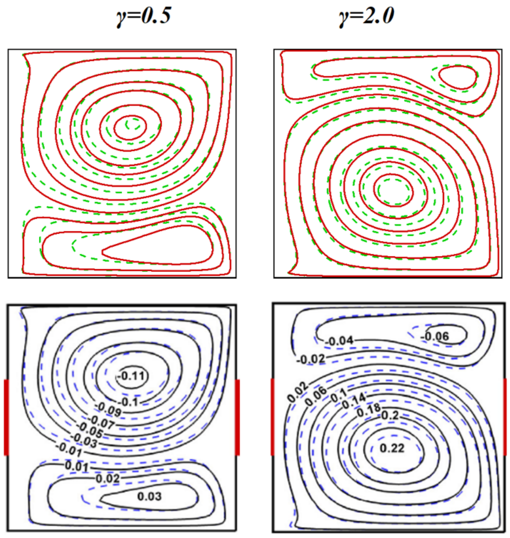

(a)

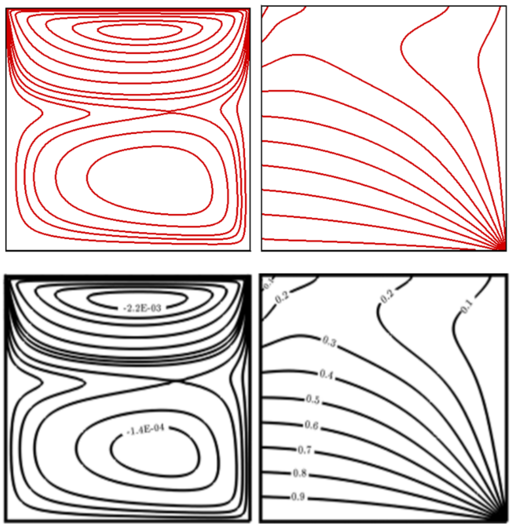

(b)

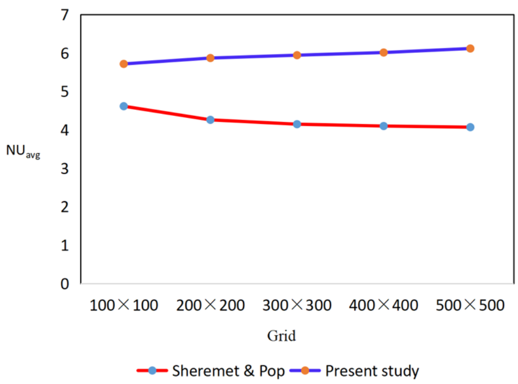

(c)

Figure 2. Comparison of (a) streamlines for various wall speed ratios with results of Jmai et al. [37] at $Ri = 1$, (b) streamlines and isotherms for $Ha = 50$ with results of Kefayati et al. [38] at $Ri = 1$, and (c) average Nusselt number values with results of Sheremet and Pop [32] at $Ri = 0.01$.

on the flow and heat transfer characteristics. The findings provide useful insights into the control of magnetohydrodynamic mixed convection and heat transfer enhancement in diagonally lid-driven nanofluid-filled cavities through appropriate selection of the wall speed ratio.

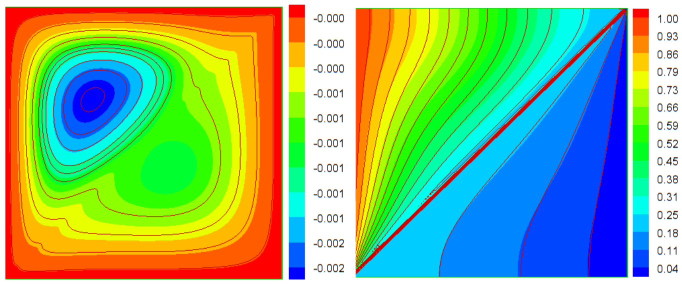

γ=0.0

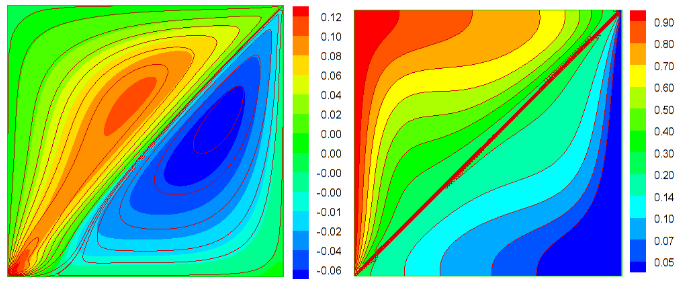

γ=1.0

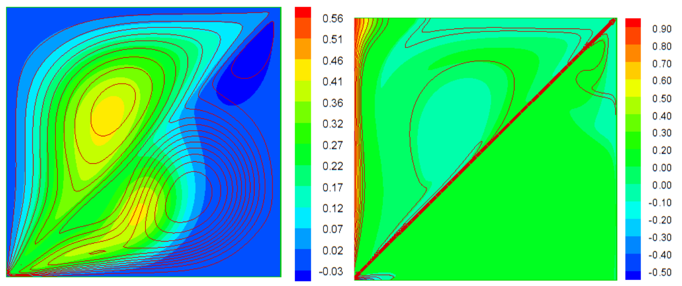

γ=2.0

Figure 3. Streamlines and isotherms for different wall speed ratios in the forced convection regime (Ri=0.1) with the heated diagonal moving wall at Ha=10.

The numerical results are presented in terms of the temperature field, flow structure, velocity distribution, and heat transfer characteristics. Figure 3 illustrates the streamlines and isotherms for different wall speed ratios under the forced convection regime ($Ri = 0.1$) with a heated diagonally moving wall.

For $\gamma = 0$, only a relatively weak primary vortex is formed inside the cavity, indicating limited fluid circulation. Correspondingly, the isotherms remain nearly parallel to the heated wall, suggesting that heat transfer is dominated by thermal conduction. As the wall speed ratio increases to $\gamma = 1$, the moving wall injects additional momentum into the cavity, strengthening the primary circulation and producing a more pronounced distortion of both the streamlines and isotherms. This behavior indicates enhanced fluid mixing and a greater contribution of convective heat transfer.

When the wall speed ratio is further increased to $\gamma = 2$, the circulation becomes considerably stronger, and the streamlines exhibit greater asymmetry owing to the intensified shear generated by the moving wall. The isotherms are significantly distorted and penetrate deeper into the cavity, reflecting a thinner thermal boundary layer and more effective heat transport. Therefore, increasing the wall speed ratio enhances shear-driven circulation, promotes fluid mixing, and improves the overall heat transfer performance. Because buoyancy effects are relatively weak at $Ri = 0.1$, the flow structure is primarily governed by wall motion, making the influence of the wall speed ratio particularly significant.

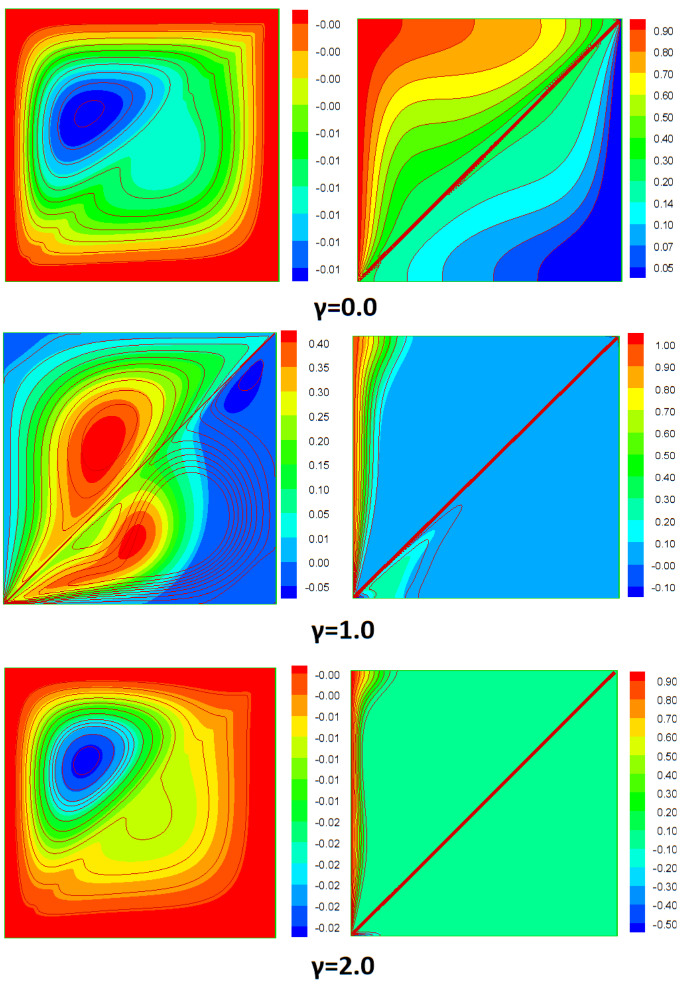

Figure 4. Streamlines and isotherms for different wall speed ratios in the mixed convection regime (Ri=1) with the heated diagonal moving wall at Ha=10.

Figure 4 presents the streamline and isotherm distributions for different wall speed ratios under the mixed convection regime ($Ri = 1$). Compared with the forced convection case, buoyancy now contributes more significantly to the flow structure, resulting in a stronger interaction between natural and forced convection.

At $\gamma = 0$, the flow remains relatively symmetric and the isotherms are only slightly distorted, indicating moderate convective transport. As the wall speed ratio increases to $\gamma = 1$, the wall motion intensifies the primary vortex and promotes stronger mixing between the fluid layers. The temperature contours become increasingly distorted, demonstrating the growing importance of convection.

For $\gamma = 2$, the streamlines become highly asymmetric and the isotherms are substantially compressed near the heated wall, indicating a marked increase in the local temperature gradient. Consequently, the convective heat transfer is significantly enhanced. These results suggest that wall motion and buoyancy jointly determine the flow behavior under mixed convection conditions, while increasing the wall speed ratio effectively reinforces the forced-convection component and improves the overall heat transfer performance.

Figure 5 presents the streamline and isotherm distributions for different wall speed ratios under the natural convection regime ($Ri = 10$). In this regime, buoyancy is the dominant driving mechanism, whereas the influence of wall motion is comparatively weaker than that observed under forced and mixed convection conditions.

At $\gamma = 0$, the flow exhibits a nearly symmetric circulation pattern, and the isotherms remain relatively smooth, indicating that heat transfer is primarily governed by buoyancy-induced convection. As the wall speed ratio increases to $\gamma = 1$, the moving wall introduces additional shear, causing the primary vortex to become asymmetric and the isotherms to deviate from their original distribution. This behavior suggests an enhancement of fluid mixing and convective heat transfer.

When the wall speed ratio is further increased to $\gamma = 2$, the streamlines become increasingly distorted, and the isotherms exhibit greater curvature and compression near the heated wall. These changes indicate stronger interaction between the shear-driven flow and the buoyancy-induced circulation, resulting in a thinner

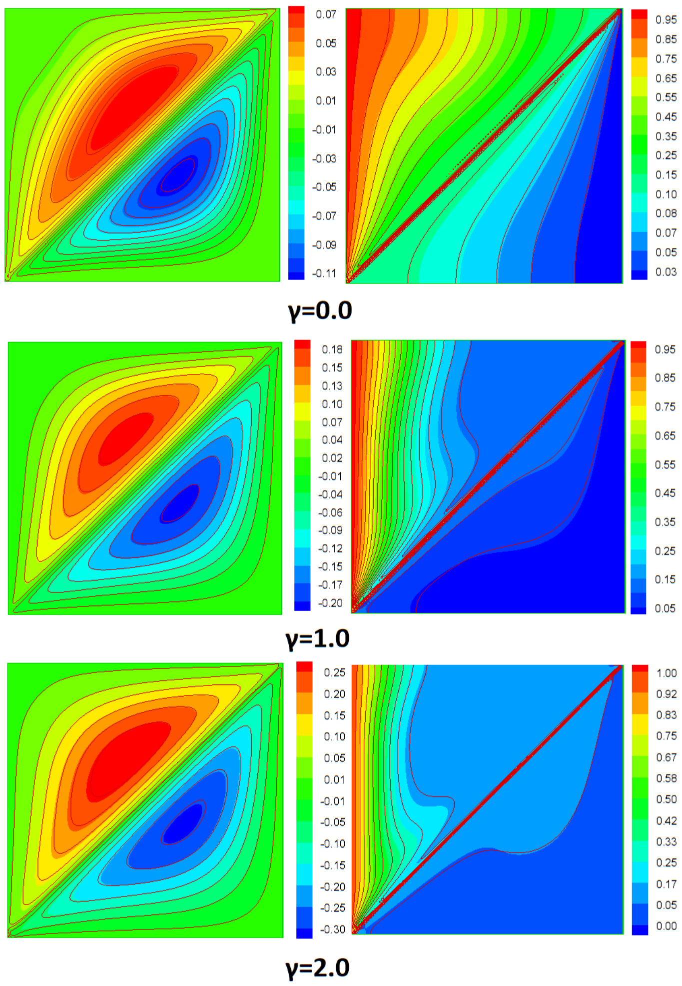

Figure 5. Streamlines and isotherms for different wall speed ratios in the natural convection regime (Ri=10) with the heated diagonal moving wall at Ha=10.

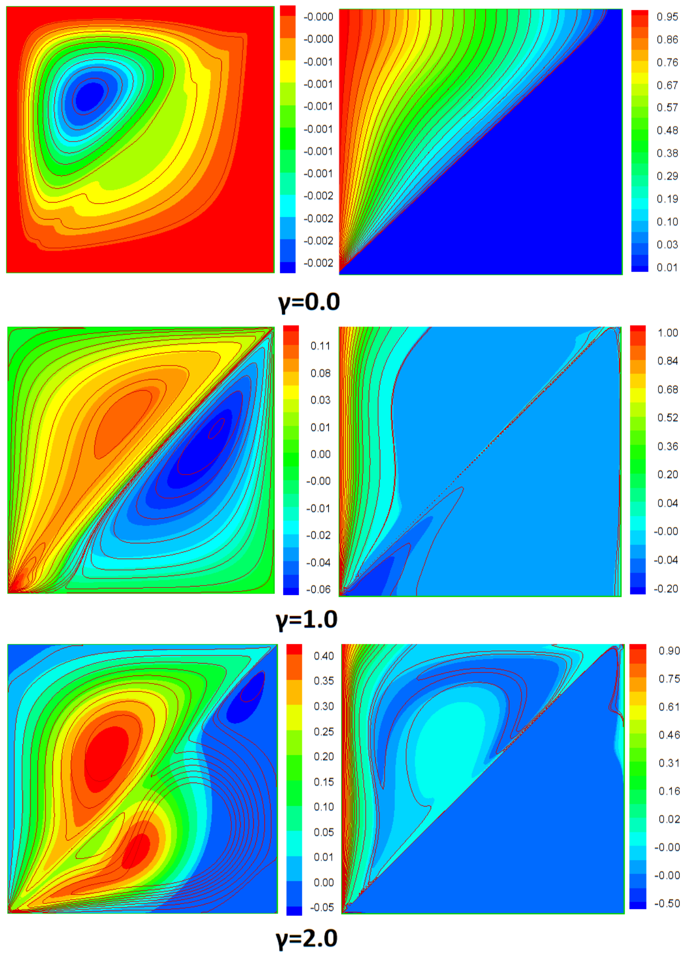

Figure 6. Streamlines and isotherms for different Hartmann numbers in the forced convection regime $(Ri = 0.1)$ with the cooled diagonal moving wall at $\gamma = 1$.

thermal boundary layer and improved heat transfer. Although natural convection remains the dominant transport mechanism, increasing the wall speed ratio still provides an effective means of enhancing fluid circulation and thermal transport.

Figure 6 illustrates the influence of the Hartmann number on the streamline and isotherm distributions under the forced convection regime $(Ri = 0.1)$. As the magnetic field strength increases, the Lorentz force suppresses fluid motion, resulting in weaker circulation and reduced mixing within the cavity.

At low Hartmann numbers, the primary vortex occupies most of the cavity, and the isotherms are noticeably distorted by the strong convective motion. As the Hartmann number increases, the circulation intensity gradually decreases and the streamlines become smoother owing to magnetic damping. Consequently, the isotherms become more parallel to the heated wall, indicating that heat transfer shifts from convection toward conduction.

These results demonstrate that the magnetic field effectively suppresses the shear-driven circulation generated by the moving wall, thereby reducing convective heat transfer under forced convection conditions.

Figure 7 presents the streamline and isotherm distributions under a stronger magnetic field. Compared with Figure 6, the suppression effect of the magnetic field becomes more pronounced as the Hartmann number increases.

At $\gamma = 0$, buoyancy dominates the flow structure and only a weak circulation is observed. Increasing the wall speed ratio strengthens the shear-driven motion; however, the enhancement is partially offset by the Lorentz force, which suppresses fluid circulation throughout the cavity. As a result, the streamlines remain smoother than those observed in the absence of a magnetic field, and the isotherms exhibit less distortion.

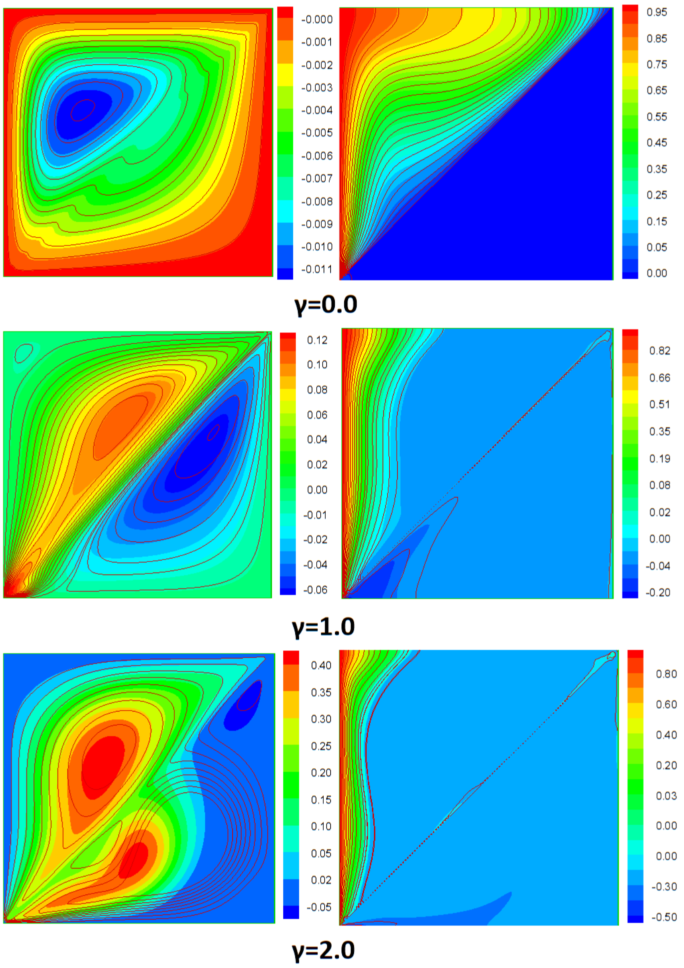

Figure 7. Streamlines and isotherms for different Hartmann numbers in the mixed convection regime ($Ri = 1$) with the cooled diagonal moving wall at $\gamma = 1$.

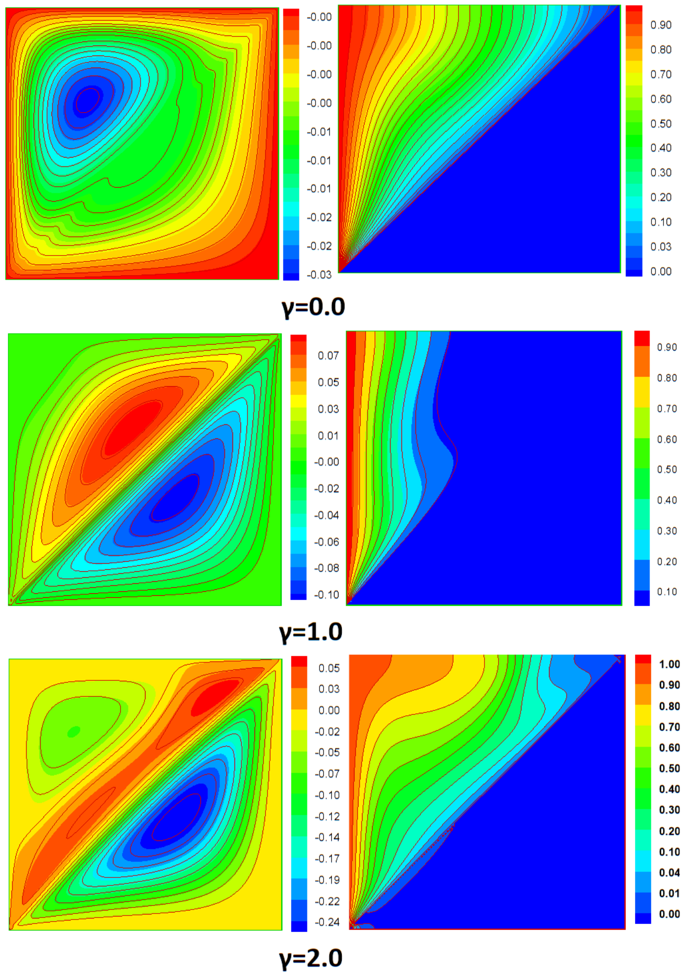

Figure 8. Streamlines and isotherms for different wall speed ratios in the natural convection regime (Ri=10) with the cooled diagonal moving wall at Ha=10.

These observations indicate that the magnetic field weakens convective transport by damping fluid motion, while increasing the wall speed ratio can only partially compensate for this suppression. Therefore, the overall heat transfer characteristics are governed by the competition between wall-induced shear and magnetic damping.

Figure 8 illustrates the influence of the wall speed ratio on magnetohydrodynamic mixed convection in a cavity with a diagonally moving cooled wall. As the wall speed ratio increases from $\gamma = 0$ to $\gamma = 2$, significant changes are observed in both the flow structure and temperature field.

At $\gamma = 0$, buoyancy dominates the flow, resulting in relatively simple streamline patterns and smooth isotherms. Increasing the wall speed ratio to $\gamma = 1$ introduces stronger shear-driven motion, leading to more intense circulation and greater distortion of the isotherms, which indicates enhanced convective transport. When the wall speed ratio is further increased to $\gamma = 2$, the streamlines become highly asymmetric and the isotherms are compressed near the moving wall, reflecting stronger fluid mixing and a thinner thermal boundary layer.

These observations indicate that the combined effects of wall motion and the magnetic field govern the flow structure, while increasing the wall speed ratio effectively enhances convective heat transfer despite the damping effect of the Lorentz force.

Figure 9 presents the variation of the average Nusselt number with the wall speed ratio for different Richardson numbers at a fixed Hartmann number ($Ha = 10$). For all Richardson numbers, the average Nusselt number increases monotonically with increasing wall speed ratio, indicating that stronger wall motion enhances convective heat transfer. The enhancement is more pronounced at higher Richardson numbers because the combined action of buoyancy and wall-induced circulation promotes more

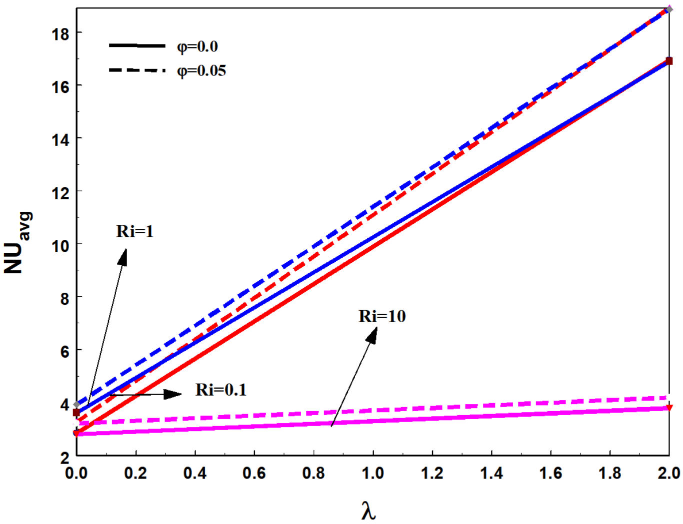

Figure 9. Average Nusselt number profiles for different Richardson number for various γ at Ha=10.

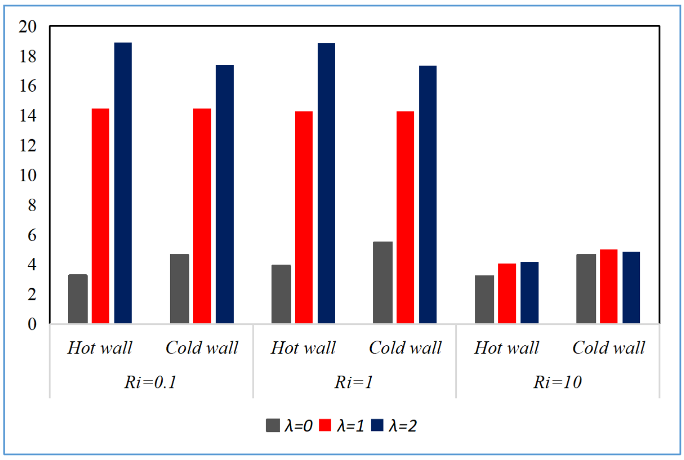

Figure 11. Average Nusselt number profiles for different Richardson number for various wall speed ratios γ at Ha=10.

efficient thermal transport.

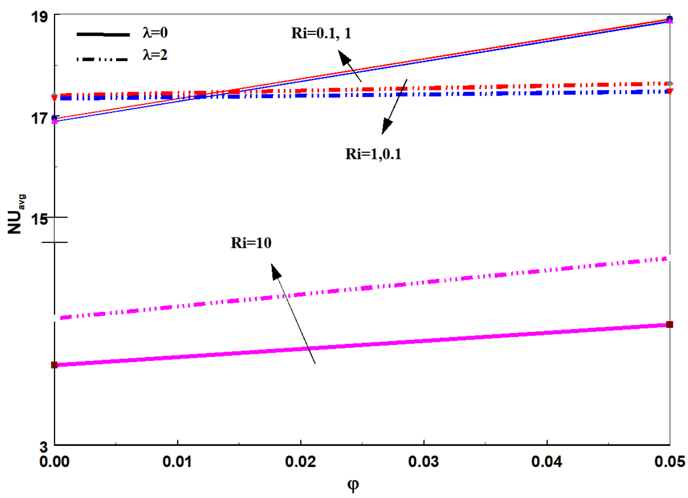

Figure 10. Average Nusselt number profiles for different Richardson number, wall speed ratios for various ϕ at Ha=10.

Figure 10 shows the effect of nanoparticle volume fraction on the average Nusselt number for different wall speed ratios. Increasing the nanoparticle volume fraction consistently enhances the average Nusselt number, particularly at larger wall speed ratios. This improvement is mainly attributed to the increased effective thermal conductivity of the nanofluid, which facilitates heat diffusion while the stronger wall motion promotes convective transport.

Figure 11 further examines the influence of the wall speed ratio on the average Nusselt number under different Richardson numbers. Increasing the wall speed ratio leads to a continuous enhancement of heat transfer, particularly at larger Richardson numbers, where the interaction between forced and natural convection becomes stronger. These results demonstrate that appropriate wall motion is an effective approach for improving the thermal performance of magnetohydrodynamic nanofluid systems.

Table 3. Average Nusselt number values for different Hartmann numbers for various Richardson numbers with $\varphi = 0.0$ and 0.05 at wall speed ratio $\gamma = 1$.

Ha	$Ri = 0.1$		$Ri = 1$		$Ri = 10$	
	$\varphi = 0$	$\varphi = 0.05$	$\varphi = 0$	$\varphi = 0.05$	$\varphi = 0$	$\varphi = 0.05$
0	20.1639	22.3784	19.6800	23.0142	4.8412	5.6321
10	19.9053	22.1278	19.3636	22.7344	4.7512	5.5080
25	18.9248	19.0718	18.2030	21.5651	4.7053	5.4758
50	18.0583	18.7144	17.5739	20.2809	4.3568	5.1632

Table 3 summarizes the average Nusselt numbers for different nanoparticle volume fractions, Hartmann numbers, and Richardson numbers at a fixed wall speed ratio of $\gamma = 1$. Several key trends can be observed from the data.

First, increasing the Hartmann number suppresses fluid circulation through the Lorentz force, thereby reducing the average Nusselt number across all cases. For example, at $Ri = 0.1$ and $\phi = 0$, increasing Ha from 0 to 50 reduces $\overline{Nu}_{avg}$ from 20.1639 to 18.0583, corresponding to a decrease of approximately 10.4%.

Second, increasing the nanoparticle volume fraction from $\phi = 0$ to $\phi = 0.05$ consistently enhances heat transfer due to the higher effective thermal conductivity of the nanofluid. At $Ha = 10$ and $Ri = 1$, the addition of nanoparticles increases $\overline{Nu}_{avg}$ from 19.3636 to 22.7344, representing an improvement of about 17.4%.

Third, the Richardson number exhibits a more complex effect on heat transfer. At low Ri ($Ri = 0.1$), forced convection induced by wall motion dominates, resulting in relatively high Nusselt numbers. As Ri increases to 1, the contribution of buoyancy becomes comparable to forced convection, leading to a slight reduction in heat transfer. At $Ri = 10$, natural convection becomes the primary driving mechanism; however, under the present configuration with a diagonally moving heated/cooled wall, the buoyancy-driven flow may suppress the shear-driven circulation, leading to a significant decrease in the average Nusselt number. For instance, at $Ha = 0$ and $\phi = 0.05$, $\overline{Nu}_{avg}$ drops from 22.3784 at $Ri = 0.1$ to 5.6321 at $Ri = 10$.

Overall, the results demonstrate that increasing the Hartmann number suppresses convective transport, while increasing the nanoparticle volume fraction enhances thermal performance. The Richardson number modulates the relative strength of forced and natural convection, with higher Ri values generally leading to reduced heat transfer in the present diagonally moving wall configuration. The wall speed ratio and magnetic field jointly determine the optimal operating conditions for maximizing heat transfer efficiency.

5 Conclusions

In this study, magnetohydrodynamic (MHD) mixed convection in a nanofluid-filled square cavity with a diagonally moving heated/cooled wall was numerically investigated. The coupled effects of the wall speed ratio, Richardson number, Hartmann number, and nanoparticle volume fraction on the flow structure and heat transfer characteristics were systematically examined.

The main conclusions are summarized as follows:

- Increasing the wall speed ratio is the most effective approach for enhancing heat transfer. Under forced convection ($Ri = 0.1$), the average Nusselt number at the heated wall increases from 3.3 to 19.0 (approximately 476%) as the wall speed ratio increases from $\gamma = 0$ to $\gamma = 2$. This enhancement is accompanied by stronger circulation and greater distortion of the isotherms, indicating more effective convective transport.
- The influence of wall motion gradually decreases as the Richardson number increases. At $\gamma = 2$, the average Nusselt number decreases from 19.0 at $Ri = 0.1$ to 4.1 at $Ri = 10$, demonstrating that buoyancy progressively dominates the flow and weakens the contribution of wall-driven convection.
- Increasing the Hartmann number suppresses fluid circulation owing to the damping effect of the Lorentz force, resulting in a reduction in heat transfer. For $Ri = 0.1$ and $\phi = 0$, increasing the Hartmann number from 0 to 25 reduces the average Nusselt number from 20.16 to 18.92.
- Increasing the nanoparticle volume fraction enhances the thermal performance of the cavity. For $Ri = 0.1$ and $Ha = 0$, increasing ϕ from 0 to 0.05 raises the average Nusselt number from 20.16 to 22.38, corresponding to an enhancement of approximately 11% owing to the higher effective thermal conductivity of the nanofluid.

Overall, the thermal performance of the cavity is governed by the competition between wall-induced shear, buoyancy, and magnetic damping. Appropriate wall motion and nanoparticle loading can enhance the effective thermal conductivity of the nanofluid, which facilitates heat diffusion and improves overall thermal performance.

Future work will focus on extending the present model to three-dimensional configurations, transient MHD mixed convection, and hybrid nanofluids, as well as experimental validation of the numerical predictions.

Data Availability Statement

Data will be made available on request.

Funding

This work was supported without any funding.

Conflicts of Interest

Muhammad Ijaz Khan served as an Editor-in-Chief of the *International Journal of Thermo-Fluid Systems and Sustainable Energy* at the time of manuscript submission. To ensure the integrity of the peer-review process, Muhammad Ijaz Khan was not involved in the editorial handling, peer review, or decision-making process for this manuscript, which was handled independently by another editor. The remaining authors declare no conflicts of interest.

AI Use Statement

The authors declare that no generative AI was used in the preparation of this manuscript.

Ethical Approval and Consent to Participate

Not applicable.

References

[1] Selimefendigil, F., & Öztop, H. F. (2014). Numerical study of MHD mixed convection in a nanofluid filled lid driven square enclosure with a rotating cylinder. *International journal of heat and mass transfer, 78*, 741-754. [CrossRef]

[2] Gibanov, N. S., Sheremet, M. A., Oztop, H. F., & Abu-Hamdeh, N. (2017). Effect of uniform inclined magnetic field on mixed convection in a lid-driven cavity having a horizontal porous layer saturated with a ferrofluid. *International Journal of Heat and Mass Transfer, 114*, 1086-1097. [CrossRef]

[3] Alsabery, A. I., Ismael, M. A., Chamkha, A. J., & Hashim, I. (2019). Effects of two-phase nanofluid model on MHD mixed convection in a lid-driven cavity in the presence of conductive inner block and corner heater. *Journal of Thermal Analysis and Calorimetry, 135*(1), 729-750. [CrossRef]

[4] Begum, A. S., Sarhan, N. M., Shomurotova, S., & Khan, M. I. (2026). Computational study of magnetohydrodynamic mixed convective flow in a nanofluid-filled cavity with diagonally moving lid. *Numerical Heat Transfer, Part A: Applications, 87*(1), 2368753. [CrossRef]

[5] Selimefendigil, F., & Öztop, H. F. (2018). Modeling and optimization of MHD mixed convection in a lid-driven trapezoidal cavity filled with alumina–water nanofluid: effects of electrical conductivity models. *International Journal of Mechanical Sciences, 136*, 264-278. [CrossRef]

[6] Nithyadevi, N., Begum, A. S., Oztop, H. F., & Abu-Hamdeh, N. (2017). Mixed convection analysis in heat transfer enhancement of a nanofluid filled porous enclosure with various wall speed ratios. *International Journal of Heat and Mass Transfer, 113*, 716-729. [CrossRef]

[7] Bahoum, A., Hattab, M. El., & Hammami, Y. El. (2025). Numerical Investigation of Mixed MHD convection in a lid-driven cubic cavity with a hybrid nanofluid. *Thermal Science, 29*(4), 2713–2728. [CrossRef]

[8] Toghraie, D. (2020). Numerical simulation on MHD mixed convection of Cu-water nanofluid in a trapezoidal lid-driven cavity. *International Journal of Applied Electromagnetics and Mechanics, 62*(4), 683-710. [CrossRef]

[9] Hosseinzadeh, K., Roghani, S., Mogharrebi, A. R., Asadi, A., & Ganji, D. D. (2021). Optimization of hybrid nanoparticles with mixture fluid flow in an octagonal porous medium by effect of radiation and magnetic field. *Journal of Thermal Analysis and Calorimetry, 143*(2), 1413-1424. [CrossRef]

[10] Oztop, H. F., Al-Salem, K., & Pop, I. (2011). MHD mixed convection in a lid-driven cavity with corner heater. *International Journal of Heat and Mass Transfer, 54*(15-16), 3494-3504. [CrossRef]

[11] Hussain, S., Mehmood, K., & Sagheer, M. (2016). MHD mixed convection and entropy generation of water–alumina nanofluid flow in a double lid driven cavity with discrete heating. *Journal of Magnetism and Magnetic Materials, 419*, 140-155. [CrossRef]

[12] Shah, I. A., Bilal, S., Asjad, M. I., & Tag-ElDin, E. M. (2022). Convective Heat and Mass Transport in Casson Fluid Flow in Curved Corrugated Cavity with Inclined Magnetic Field. *Micromachines 2022, 13*, 1624. [CrossRef]

[13] Mehmood, K., Hussain, S., & Sagheer, M. (2017). Numerical simulation of MHD mixed convection in alumina–water nanofluid filled square porous cavity using KKL model: Effects of non-linear thermal radiation and inclined magnetic field. *Journal of Molecular Liquids, 238*, 485-498. [CrossRef]

[14] Hussain, S., Ahmad, S., Mehmood, K., & Sagheer, M. (2017). Effects of inclination angle on mixed convective nanofluid flow in a double lid-driven cavity with discrete heat sources. *International Journal of Heat and Mass Transfer, 106*, 847-860. [CrossRef]

[15] Kattimani, P., Sollapur, S. B., Kedia, A., Singh, K., & Sarris, I. E. (2026). The role of high-oscillating magnetic field dynamics in nanofluid flow. *Nano, 21*(07), 2550101. [CrossRef]

[16] Asghar, A., Chandio, A. F., Shah, Z., Vrinceanu, N., Deebani, W., Shutaywi, M., & Lund, L. A. (2023). Magnetized mixed convection hybrid nanofluid with effect of heat generation/absorption and velocity slip condition. *Heliyon, 9*(2). [CrossRef]

[17] Sivasankaran, S., Malleswaran, A., Lee, J., & Sundar, P. (2011). Hydro-magnetic combined convection in a lid-driven cavity with sinusoidal boundary conditions on both sidewalls. *International Journal of Heat and Mass Transfer, 54*(1-3), 512-525. [CrossRef]

[18] Sheikholeslami, M., Bandpy, M. G., Ellahi, R., & Zeeshan, A. (2014). Simulation of MHD CuO–water nanofluid flow and convective heat transfer considering Lorentz forces. *Journal of Magnetism and Magnetic Materials, 369*, 69-80. [CrossRef]

[19] Elshehabey, H. M., & Ahmed, S. E. (2015). MHD mixed convection in a lid-driven cavity filled by a nanofluid with sinusoidal temperature distribution on the both vertical walls using Buongiorno's nanofluid model. *International Journal of Heat and Mass Transfer, 88*, 181-202. [CrossRef]

[20] Begum, A. S., Nithyadevi, N., Öztop, H. F., & Al-Salem, K. (2017). Numerical simulation of MHD mixed convection in a nanofluid filled non-Darcy porous

enclosure. *International Journal of Mechanical Sciences, 130*, 154-166. [CrossRef]

[21] Nithyadevi, N., & Begum, A. S. (2018). Numerical study on the effect of magnetic field in a porous enclosure using nanofluid with mid-horizontal moving lid: Brinkman-Forchheimer extended darcy model. *Journal of Porous Media, 21*(5), 457–470. [CrossRef]

[22] Taamneh, Y., & Bataineh, K. (2017). Mixed Convection Heat Transfer in a Square Lid-Driven Cavity Filled with Al_2O_3-Water Nanofluid. *Journal of Mechanical Engineering/Strojniški Vestnik, 63*(6), 383. [CrossRef]

[23] Chowdhury, K., & Alim, M. A. (2023). Mixed Convection in a Double Lid-Driven Wavy Shaped Cavity Filled with Nanofluid Subject to Magnetic Field and Internal Heat Source. *Journal of Applied Mathematics, 2023*(1), 7117186. [CrossRef]

[24] Hanif, H., Shafie, S., & Jagun, Z. T. (2024). Maximizing thermal efficiency of a cavity using hybrid nanofluid. *Journal of Cleaner Production, 441*, 141089. [CrossRef]

[25] Sarlak, R., Abed, A. M., Akbari, O. A., Marzban, A., Baghaei, S., & Bayat, M. (2023). Numerical investigation of natural convection heat transfer of water/SWCNT nanofluid flow in a triangular cavity with cold fluid injection. *Progress in Nuclear Energy, 155*, 104513. [CrossRef]

[26] Chamkha, A. J., & Abu-Nada, E. (2012). Mixed convection flow in single- and double-lid driven square cavities filled with water-Al2O3 nanofluid: effects of viscosity models. *European Journal of Mechanics - B/Fluids, 36*, 82–96. [CrossRef]

[27] Nazir, M. W., Javed, T., Ali, N., & Nazeer, M. (2024). Effects of radiative heat flux and heat generation on magnetohydrodynamics natural convection flow of nanofluid inside a porous triangular cavity with thermal boundary conditions. *Numerical Methods for Partial Differential Equations, 40*(2), e22768. [CrossRef]

[28] Qureshi, M. A., Hussain, S., & Sadiq, M. A. (2021). Numerical simulations of MHD mixed convection of hybrid nanofluid flow in a horizontal channel with cavity: Impact on heat transfer and hydrodynamic forces. *Case Studies in Thermal Engineering, 27*, 101321. [CrossRef]

[29] Gowthaman, D., Ali, A. B., Begum, A. S., Jayasimman, I. P., Al-Harbi, F. F., Jameel, M., ... & Ali, S. (2025). Shear-and buoyancy-dominated heat transfer: Influence of plate speed and nanoparticles. *International Communications in Heat and Mass Transfer, 169*, 109787. [CrossRef]

[30] Selimefendigil, F., Öztop, H. F., & Chamkha, A. J. (2016). MHD mixed convection and entropy generation of nanofluid filled lid driven cavity under the influence of inclined magnetic fields imposed to its upper and lower diagonal triangular domains. *Journal of Magnetism and Magnetic Materials, 406*, 266-281. [CrossRef]

[31] Abu-Nada, E., & Oztop, H. F. (2009). Effects of inclination angle on natural convection in enclosures filled with Cu–water nanofluid. *International journal of heat and fluid flow, 30*(4), 669-678. [CrossRef]

[32] Sheremet, M. A., & Pop, I. (2015). Mixed convection in a lid-driven square cavity filled by a nanofluid: Buongiorno's mathematical model. *Applied Mathematics and Computation, 266*, 792-808. [CrossRef]

[33] Koo, J., & Kleinstreuer, C. (2005). Laminar nanofluid flow in microheat-sinks. *International journal of heat and mass transfer, 48*(13), 2652-2661. [CrossRef]

[34] Garnett, J. M. (1904). Colours in metal glasses and in metallic films. *Philosophical Transactions of the Royal Society of London. Series A, Containing Papers of a Mathematical or Physical Character*, 385-420. https://www.jstor.org/stable/90866

[35] Vajjha, R. S., & Das, D. K. (2009). Experimental determination of thermal conductivity of three nanofluids and development of new correlations. *International journal of heat and mass transfer, 52*(21-22), 4675-4682. [CrossRef]

[36] Patankar, S. V. (1980). *Numerical Heat Transfer and Fluid Flow*. Hemisphere Publishing Corporation. [CrossRef]

[37] Jmai, R., Ben-Beya, B., & Lili, T. (2016). Numerical analysis of mixed convection at various walls speed ratios in two-sided lid-driven cavity partially heated and filled with nanofluid. *Journal of Molecular Liquids, 221*, 691-713. [CrossRef]

[38] Kefayati, G. R., Gorji-Bandpy, M., Sajjadi, H., & Ganji, D. D. (2012). Lattice Boltzmann simulation of MHD mixed convection in a lid-driven square cavity with linearly heated wall. *Scientia Iranica, 19*(4), 1053-1065. [CrossRef]

Muhammad Ijaz Khan received MS and PhD from Quaid-I-Azam University, Islamabad, Pakistan in the year 2016 and 2019 in Applied Mathematics for work in the field of CFD analysis, Flow Behavior and Numerical techniques (AI). Currently working as Assistant Professor in the Department of Mechanical Engineering, Prince Mohammad Bin Fahd University, P. O. Box, 1664, Al-Khobar 31952, Kingdom of Saudi Arabia. Contributed more than 50 research-level papers to many International journals. Research interests include Sensor Networks, Machine Learning, and Cloud computing, Flow Behavior, CFD analysis. (Email: ijzfmg_khan@yahoo.com)